ELSEVIER

Journal of Non-Crystalline Solids 210 (1997) 70–86

JOURNAL OF NON-CRYSTALLINE SOLIDS

Possible universalities in the ac frequency response of dispersed, disordered materials

J. Ross Macdonald *

Department of Physics and Astronomy, University of North Carolina, Chapel Hill, NC 27599-3255, USA

Received 21 September 1995; revised 18 June 1996

Abstract

The plausibility of recent suggestions that the electrical conductivity of crystalline and glassy disordered materials may often arise from two separate physical processes, each involving dispersed response, is examined by means of a detailed, complex-non-linear-least-squares analysis of small-signal frequency-response data on $CaTiO_3$:30%Al^{3+} over a temperature range from 51 to 626 K. Earlier preliminary analysis on a few of the available 16 data sets, which showed that they could indeed be described by a combination of conductive-system dispersion and dielectric-system dispersion, is confirmed and extended. Complex non-linear least squares analysis provides a high-resolution method of isolating, identifying, and examining these separate response contributions. It was found that the conductive-system part of the full response could be well represented over a wide temperature range by a power-law model with an exponent close to 0.5, suggesting the presence of diffusion. A new analysis procedure showed that the relaxation time and dc conductivity exhibited the same thermally activated temperature response with no pre-exponential T dependence. The dielectric-system dispersion was well described by a thermally activated exponential-distribution-of-activation-energies model, whose effective power-law exponent exhibited $[1-(T/T_0)]$ temperature dependence from 51 to 296 K. Thus, when the present analysis methods were applied to these data, the constant-loss 'second universality', found earlier for this and other materials, one which involves a power-law exponent of unity, did not appear in the 64 to 224 K region where it was previously identified for the present material.

1. Introduction and background

Several kinds of universal, small-signal, electrical ac frequency responses have been proposed over the years for materials exhibiting dispersive behavior [1–6]. They all involve consideration of the log–log slope, s, of the real part of the complex conductivity or admittance, usually described by the exponent γ in a power-law response model involving ω^{γ}. Thus, if the complex conductivity is written as $\sigma(\omega) = \sigma'(\omega) + i\sigma''(\omega)$, with $\sigma'(0) \equiv \sigma_0$ and $\Delta\sigma(\omega) \equiv \sigma'(\omega) - \sigma'(0)$, then s is defined as $\mathrm{d}\ln[\Delta\sigma(\omega)/\sigma_n]/\mathrm{d}\ln[\omega/\omega_0]$. Here, $i \equiv \sqrt{-1}$, σ_n and ω_0 are normalization constants of magnitude unity, and we shall use just 'slope' to mean s hereafter. Although s is usually taken to be frequency independent over an appreciable frequency range (e.g., one involving a decade or more), it need not be. It is only when it is independent, however, that it is reasonable to set s and γ equal. Although the symbol 's' is frequently used for a power-law

* Corresponding author. Tel.: +1-919 967 5005; fax: +1-919 962 0480; e-mail: macd@gibbs.oit.unc.edu.

PII S0022-3093(96)00564-9

exponent, it is better to use a different symbol, such as the present γ, to avoid confusion between slope and exponent quantities. Estimated exponent values are always averages over the data considered. When s or γ is independent of temperature over a significant temperature range (e.g., one from T to $\sim 2T$ or more), they will be denoted as s_0 or γ_0. The complex resistivity is $\rho(\omega) = [\sigma(\omega)]^{-1} = \rho'(\omega) + i\rho''(\omega)$. A list of acronyms used herein appears at the end of this work.

The earliest and most common universality is that involving fractional-exponent, power-law response, where $0 < \gamma < 1$. Such response, with $\gamma = \gamma_0$, was publicized by Jonscher and called universal dielectric response [1,2], but more recently it has been termed universal dynamic response [3], making it clearer that it may appear in the response of either dielectric or conducting systems. Fractional power-law response is actually implicit, however, in the 1854 work of Kohlrausch on stretched exponential behavior [4]. At the conductivity level it may be written as

$$\sigma'_{ac}(\omega) \equiv \Delta\sigma(\omega) = A\omega^{\gamma}, \tag{1}$$

where A is frequency-independent.

In 1991, Lee, Liu and Nowick [5] proposed an important 'new universality' in the frequency response of ionically conducting crystals and glasses, namely that, for a variety of data on different materials over a range of relatively low temperatures (as large as 95 to 400 K or 64 to 224 K [6]) $\gamma = \gamma_0 = 1$, disagreeing with many theoretical predictions concerned with dielectric dispersion that, as the temperature T approaches zero,

$$\gamma = 1 - (T/T_0), \tag{2}$$

where T_0 is a constant temperature [7–12]. The $\gamma_0 = 1$ result implies the existence of a frequency-independent loss represented by the quantity $\Delta\epsilon''(\omega) = \Delta\sigma(\omega)/(\omega\epsilon_V)$, where ϵ_V is the permittivity of vacuum. Here the complex dielectric constant is defined as $\epsilon(\omega) = \epsilon'(\omega) - i\epsilon''(\omega) = \sigma(\omega)/(i\omega\epsilon_V)$. It is worth noting that although Lee, Liu and Nowick were not the first to publish results indicating $\gamma_0 \geq 1$ (e.g., [13,14], and references therein), they were perhaps the first to explicitly identify it as a new or second universality.

Doubt has been cast on the appropriateness of the constant-loss phenomenon by the results of my re-analysis of two sets of data used by Nowick and his collaborators [5,6]: that for NaCl doped with Zn^{2+} [15] and that for $CaTiO_3$:30%Al^{3+} [16]. It has been stated by Nowick and associates that the former material is a poor example for testing the hypothesis because subsequent measurements over the original temperature range did not verify it because of sample aging [17]. Such aging is not necessarily relevant to the original data [5] nor to the novel and self-consistent results of their analysis [15]. In fact, as discussed below, the issue primarily involves differences in methods of data analysis for the same data, rather than differences in the data. The question of the existence of distinct constant-loss behavior in $CaTiO_3$:30%Al^{3+} [16–18] is further addressed herein. Further, the purpose of the present work is not to show that constant-loss behavior may not occur, but to demonstrate that careful data analysis may not always verify previous conclusions that it does.

An additional feature of the work of Nowick and associates is that they found for temperatures appreciably greater than those where they concluded that an exponent of unity applied, that γ decreased to a final high-temperature limiting value, γ_0, of about 0.5 to 0.6 [5,6,17,18]. Later [6] they proposed that instead of considering only a model involving a single γ as a continuous function of temperature, $\gamma(T)$ such behavior might alternatively be expressed by the double-power-law response model,

$$\sigma'(\omega) = \sigma'(0) + A\omega^{\gamma_0} + B\omega^{1}, \tag{3}$$

where A is thermally activated; B involves only small temperature dependence; and $\gamma_0 \simeq 0.6$. Such combined response may be considered a possible third kind of universal response.

Socrates said: "The unexamined life is not worth living". Similarly, it is not much of an exaggeration to say, "an inadequately analyzed data set is not worth generating". The main aim of the present work is to re-analyze the $CaTiO_3$:30%Al^{3+} data of Nowick and associates using more objective and powerful methods than those authors employed. Is it possible, through the use of complex non-linear least squares (CNLS) fitting methods and more appropriate fitting models, to obtain new results significantly different and more precise than those of Nowick and associates, and, thereby, gain new physical insights

into the electrical behavior of this material? I believe that the results of the present work demonstrate that it is indeed possible, and, in doing so, they illustrate the utility of the analysis methods employed.

Nowick and associates rewrote their Eq. (3) in the equivalent form

$$\sigma'(\omega) = \sigma'(0)\left[1 + (\omega\tau)^{\gamma_0}\right] + B\omega^1, \qquad (4)$$

representing the superposition of two types of response regimes [18]. The first term on the right was defined as leading to the Jonscher regime and the second as that associated with the constant-loss regime. One of the objects of the present work is to use high-resolution CNLS data analysis methods to evaluate the applicability of such a two-regime representation and to distinguish between true $\gamma(T)$ response involving a single phenomenon and that arising from the presence of two separate physical mechanisms. Note that Eqs. (3) and (4) suggest that the two responses are present over the entire frequency range for any measuring temperature, though one or the other will be dominant in different temperature ranges.

In fact, Nowick and associates found that the A term in Eq. (3) was dominant only in the high temperature region and the B term only at low temperatures and high frequencies. Later, Elliott [19] termed such behavior Type I (high T, low ω) and Type II (low T, high ω with $\gamma \geq 1$). This classification is reminiscent of an earlier, somewhat more general one [12,15,16,20] which includes it. The more general approach proposes that the overall behavior of a glass or other disordered material exhibiting dispersed frequency response is often made up of two separate and independent dispersion processes whose contributions are electrically in parallel. The first one is associated with charge carriers whose motion can contribute to dc conduction and dispersive ac response, often by hopping, and is designated conductive-system dispersion (CSD). For such response, a single process leads to both ac and dc behavior.

The second process, termed dielectric-system dispersion (DSD), is associated with the presence of induced or permanent dipoles (conventional dielectric behavior) and/or with the motion of non-percolating charges, for example ones associated with localized hopping back and forth in an asymmetric double well potential configuration, either by surmounting a potential barrier separating the two sites [21,22] and/or by tunneling through the barrier [23]. It is consistent with the above definitions to identify the Type I behavior exemplified by the A term in Eq. (3) with CSD and the B term with DSD, but it should be remembered that in general CSD and DSD responses need not be of the forms of those proposed in Eq. (3) or Eq. (4). Note that even in the absence of any DSD a high-frequency-limiting dielectric constant, $\epsilon'_D(\infty) \equiv \epsilon_{D\infty}$, will always be present. Here the subscript 'D' denotes that $\epsilon_{D\infty}$ is associated only with conventional bulk dielectric effects and may be different from the measured ϵ_∞.

Recently Sidebottom, Green and Brow [24] published frequency response data for alkali oxide glasses which show $\gamma(T)$ dependence similar to that found by Nowick and associates, including $\gamma_0 = 1$ at lower temperatures. Sidebottom et al. presented few analysis results, but they emphasized that their data could be best represented by the superposition of two power laws involving different physical processes. They did not point out that this conclusion was not novel but is implicit or explicit in the earlier work of Nowick and associates and others [6,12,15,18,25]. Sidebottom et al. ascribed their DSD-type response to the limited motion of non-bridging oxygens [19] present in their materials, behavior not directly related to the CSD response associated with long-range ion motion.

In addition to possible universal response involving the effects of CSD and DSD simultaneously present, Dyre [26] has proposed that an effective-medium model originally published by Bryksin [27] leads to universal CSD behavior. This model was later generalized [28] to include explicit temperature dependence, and it has been called the GBEM equation (see acronym list). A simplified version of the GBEM model was termed the BDM equation [16,20]. Although later work [16,28] raises doubt about the universality of any of these equations, they certainly warrant continued comparison with experimental results. It is important to note that although the GBEM model does not involve any explicit fractional exponent, such as that present in Eqs. (3) and (4) and most other response models, it nevertheless leads to similar $\gamma(T)$ behavior.

One result of the above work was the derivation

of a somewhat modified type of Arrhenius activation relation which may possibly be applicable to thermally activated CSD behavior. Assume that there is a distribution of free-energy barriers present which is associated with a distribution of activation energies (actually enthalpies), E. Then the relaxation time may be written as usual as

$$\tau = \tau_a \exp(E/k_B T), \tag{5}$$

where τ_a is the inverse of a barrier attempt frequency, one which is usually larger than 10^{12} s^{-1} [29], and k_B is the Boltzmann constant. Finally, define E_H as the maximum barrier height, take the minimum height as zero, and let

$$\tau_C \equiv \tau_a \exp(E_H/k_B T). \tag{6}$$

Then for an exponential distribution of activation energies (EDAE), it has been proposed that [28]

$$\rho'(0) = (\tau_a/\epsilon_V)(k_B T/E_H)\{\exp(E_H/k_B T) - 1\}. \tag{7}$$

Notice the presence of T in the pre-exponential factor and that $\rho'(0)$ reduces to the temperature-independent or, at most, weakly temperature-dependent value τ_a/ϵ_V when $E_H/T \to 0$. Finally, a more general expression for $\rho'(0)$, involving an activation energy, E_ρ, not necessarily equal to E_H, may be written as

$$\rho'(0) = (\tau_a/\epsilon_V K_C)\exp(E_\rho/k_B T), \tag{8}$$

where K_C is a dimensionless quantity which may be temperature-dependent but not thermally activated.

2. Fitting models

2.1. Full CSD and DSD response

If one accepts the possibility that the data of Nowick et al. and that of Sidebottom et al. involve CSD and DSD contributions, as well as possible electrode effects, $\sigma_{el}(\omega)$, then the overall response at the complex conductivity level may be written in general terms as [12,16,20]

$$\sigma(\omega) = \sigma_S(\omega)/[1 + \{\sigma_S(\omega)/\sigma_{el}(\omega)\}], \tag{9}$$

where $\sigma_S(\omega) \equiv \sigma_C(\omega) + \sigma_D(\omega)$, and the 'C' and 'D' subscripts identify CSD and DSD response terms, respectively. Note that this general fitting model involves all complex quantities, does not deal only with $\sigma'(\omega)$, and still is sufficiently general that it does not beg the question of whether the DSD term in Eqs. (3) and (4) involves just $\gamma_0 = 1$.

Although Lim et al. [6] have stated that $\epsilon'(\omega)$ data (corresponding to $\sigma''(\omega)$) are relatively uninteresting, this opinion should not be accepted because the conventional approach of measuring the complex conductance but analyzing only the real part of the resulting complex conductivity is generally inadequate and inappropriate. Simultaneous fitting of both the real and imaginary part of data to an appropriate model is always superior to that of either separately, not only because it leads to better error averaging, but also because both parts of the data must simultaneously fit a model which satisfies the Kronig–Kramers relations [30,31].

Even though the real and imaginary parts of $\sigma(\omega)$, as well as all of the individual dispersive parts of the quantities present in Eq. (9), must satisfy the Kronig–Kramers relations, the exact real-parts of different response models may be so similar that even noise-free responses cannot be distinguished over a finite but wide range of ω on a log–log plot of $\sigma'(\omega)$ versus ω [32]. The frequency dependencies of the imaginary parts of the response of two such models may be appreciably different within the measurement frequency window. Since model discrimination using real-part fitting alone can, nevertheless, be carried out unambiguously for data with sufficiently low noise which extends over a sufficiently wide range of frequencies (the Kronig–Kramers relations require an infinite range), clearly the conventional approach is adequate for data of sufficiently low errors and wide range. When such data are unavailable, the usual situation, the ability to distinguish between two such models with the available imperfect data is greatly improved when the data are fitted to the models using CNLS fitting. Here such fitting is carried out using the general program LEVM with proportional weighing [33] [1]. Finally, since no exact imaginary-part response is

[1] Version 6.1 of the LEVM fitting program may be obtained at no cost from Solartron Instruments, Farnborough, Hampshire, GU14 7PW, UK, attention Dave Bartram, e-mail: bartram@solartron.com.

available for the Nowick and associates real-part responses of Eqs. (3) and (4), fully complex fitting models are required for CNLS fitting of the present data.

2.2. Conductive-system response

Although the first term on the right of Eq. (4), first suggested by Almond and West [34], has been widely used for real-part data analysis, it is not exactly the real part of an appropriate Kronig–Kramers pair, and its interpretation has been criticized [35,36]. A more appropriate empirical CSD response model is that introduced by Havriliak and Negami [37]

$$\sigma_C(\omega) = \sigma'(0)\left[1 + (i\omega\tau_C)^{\gamma}\right]^{\beta}, \tag{10}$$

where $0 < \gamma$, $\gamma\beta \leq 1$, and γ and β are frequency independent. Even though this model is not physically realizable because it predicts infinite $\sigma'_C(\omega)$ in the limit of high frequencies (unless $\gamma = \beta = 1$) [38], it is still useful in many situations because the region where $\sigma'_C(\omega)$ data must approach a constant value often appears far beyond the highest measurement frequency. Eq. (10) with $\gamma < 1$ is also non-physical in the $\omega \to 0$ limit for any value of β, but this is not the case when $\gamma = 1$. Physical realizability can be ensured by truncation of the distribution of relaxation times associated with Eq. (10) response, but such truncation is often unnecessary because of the limited frequency range of the available data.

When $\beta = 1$, the choice with which we shall be most concerned for the present CSD response regime, Eq. (10) has been named the ZC model [39], and its use for CSD data fitting predates that of the Almond–West work. When $\beta = 1$, the ac part of Eq. (10) may be written $C(i\omega)^{\gamma}$, where C is a frequency-independent parameter. This part has also been found useful for data fitting [39] and has been termed the constant-phase element (CPE).

We use the ZC model for CSD fitting in the present work because it is the complex version of the first term of Eq. (4), that used by Nowick and his associates; because it yields good fitting results with a minimum of parameters; and because it allows the present results to be directly compared to those of Nowick and his colleagues. But many more CSD fitting models are available, and a particular one should not be chosen without comparing its utility with that of others, such as, for example, the general Havriliak–Negami equation, the EDAE model (see Section 2.3), and two different stretched-exponential (Kohlrausch–Williams–Watts (KWW)) response models, KWW0 and KWW1. These KWW models both involve the slope-related exponent β. The KWW0 model amounts to using usual DSD KWW response at the impedance rather than at the complex dielectric constant level [9,40]. The second is a correction and extension [40] of the modulus formalism introduced by Moynihan and his co-workers [41,42]. Instead of involving the usual KWW distribution of relaxation times, say $g_K(\tau)$, it uses $\tau g_K(\tau)$ [9,40]. Fitting frequency response data to a KWW model by either CNLS or non-linear least squares (NLS) has been notoriously difficult because an accurate closed form-response model has been unavailable [40,43]. Recently, however, exceptionally accurate CNLS fitting routines for both models with arbitrary β have been added to the LEVM program and will be available when its next version is released in late 1996. All the models mentioned here have been used in order to help select the most appropriate one for fitting the present data, and some of their fitting results are discussed later.

When CSD response is thermally activated, the usual situation, one generally finds that the activation energy for the dc conductivity, E_σ, and that for the associated τ_C relaxation time, E_τ, are nearly identical [18,25,44], a result in agreement with the empirical Barton, Nakajima and Namikawa (BNN) relation [45–47]. This means that when parameters such as $\rho'(0) = [\sigma'(0)]^{-1}$, the dc resistivity, and τ_C are obtained by least squares fitting of data, their correlation approaches unity closely, making it difficult to obtain good estimates of the fitting parameters, their standard deviations, and their associated activation energies. It has therefore been suggested [15,40] that the τ_C in Eq. (10) and similar models be replaced by

$$\tau_C \equiv \rho'(0)\,\epsilon_V\,\epsilon_{C\tau}, \tag{11}$$

where $\epsilon_{C\tau}$ is a new dielectric constant, a quantity which will be less correlated with $\rho'(0)$, and one which should show less temperature dependence than τ_C itself when $E_\tau \simeq E_\rho$.

It turns out to be possible to give a theoretical

interpretation to the new quantity $\epsilon_{C\tau}$. Conductive-system dispersion leads to a contribution to the overall dielectric constant, $\epsilon_C(\omega)$, independent (to at least first order) of any DSD dielectric-constant contribution. Let $\epsilon_{C0} \equiv \epsilon'_C(0)$. Recent work [40] has shown that when $\rho'(\infty) = 0$, the usual situation, the BNN relation should be replaced by the first equality below

$$\tau_C/\rho'(0)\epsilon_V = (\epsilon_{C0}/\langle x\rangle) \equiv \epsilon_{C\tau} = K_C \exp\left[(E_H - E_\rho)/k_B T\right], \quad (12)$$

and Eqs. (6), (8) and (11) have been used for the rest of the expression. Here $x \equiv \tau/\tau_C$, and $\langle x\rangle$ is the first moment of the normalized, dimensionless distribution of relaxation times or activation energies that is associated with the CSD response [40]. Note that $\langle x\rangle \equiv \langle\tau\rangle/\tau_C$ depends only on the shape of the distribution rather than directly on τ_C. For example, for the Cole–Davidson model, Eq. (10) with $\gamma = 1$, $\langle x\rangle$ equals β [48]. When the temperature dependencies of $\rho'(0)$ and τ_C are exactly the same, $\epsilon_{C\tau}$ equals K_C, a temperature-independent quantity. On the other hand, if Eqs. (6) and (7) apply, $\epsilon_{C\tau}$ will be proportional to T^{-1}, while otherwise it may show thermally activated temperature dependence. Thus, direct estimation of $\epsilon_{C\tau}$ by CNLS fitting provides a sensitive test of the relation between the temperature dependencies of $\rho'(0)$ and τ_C.

It is worth mentioning that since the LEVM fitting program allows one to estimate numerically the actual distribution of activation energies associated with the available data of limited range [20,49,50], the estimated distribution can be used to estimate $\langle x\rangle$ at each temperature, allowing $\epsilon_{C0}(T)$ to then be estimated, especially valuable when insufficient low-frequency data is available to allow its direct estimate.

2.3. Dielectric-system response

Finding an adequate replacement for the DSD $B\omega$ term in Eqs. (3) and (4) is not entirely straightforward. First, one needs an equation whose real part can yield a value of s_0 not only of unity over an appreciable frequency range, but, for generality, also values either less than or greater than 1. The corresponding exponent of $\Delta\epsilon''(\omega)$ can then run from positive to negative. Although the CPR might be thought to be useful, it degenerates to a pure capacitance for $\gamma = 1$ and to a pure conductance for $\gamma = 0$ thus, it does not yield a real part like $B\omega$ and an imaginary one. Further, the long-known, approximate Kronig–Kramers relation used by Nowick et al. [17] to obtain an estimate of $\Delta\epsilon''(\omega)$ from $\epsilon'(\omega)$ data is often too inaccurate [50], is unnecessary with CNLS fitting, and is inappropriate for fitting purposes in any event.

Prior work indicates, however, that the above requirements are well met by the EDAE response model. Although such a distribution has been primarily used in the past to fit CSD impedance spectroscopy data [12,20,39,51], it has been shown in Ref. [9] that any CSD model can be formally transformed to a corresponding DSD model. Further, Wang and Bates [22] have demonstrated that a double-potential-well model can lead to EDAE response of DSD type. Therefore, an EDAE model will be used here to represent the DSD part of the complete response. Let $u_H \equiv E_H/k_B T$ and $\phi \equiv \phi_D$. Next, define $r \equiv \exp(u_H) \equiv \tau_D/\tau_a$ and $\Omega_D \equiv \omega\tau_D$, where τ_D is assumed to be thermally activated as in Eq. (6). Then EDAE model response may be expressed in normalized form at the complex-dielectric-constant level as

$$I_D(\Omega_D) \equiv \left[\epsilon_D(\Omega_D) - \epsilon'_D(\infty)\right] / \left[\epsilon'_D(0) - \epsilon'_D(\infty)\right], \quad (13)$$

with

$$I_D(\Omega_D) = \phi\left[1 - \exp(-\phi u_H)\right]^{-1} \int_0^{u_H} \frac{\exp(-\phi x)\,dx}{1 + i\Omega_D \exp(-x)}. \quad (14)$$

where u_H is a cut-off parameter. Here the parameter ϕ, which falls in the range $-\infty < \phi < \infty$ is closely equal to $(1 - \gamma_0)$ when $-0.5 \le \phi \le 0.5$ and $\Omega_D \gg 1$. For $|\phi| > 0.5$, s begins to become frequency dependent. When $\phi = 0$, the exponential distribution degenerates to a flat-top box distribution, one where all activation energies are equally probable.

Although Eq. (14) must be evaluated numerically for most values of ϕ [9], it is incorporated as a fitting model in LEVM and so may readily be used

for any ϕ. When $\phi = 0$, however, a closed-form result is available [9,20], namely

$$I_D(\Omega_D) = 1 - u_H^{-1} \ln[(1 + i\Omega_D)/(1 + i\Omega_D r^{-1})]. \quad (15)$$

For $r \gg 1$, the usual situation, and $\Omega_D \gg 1$, the imaginary part of Eq. (15) leads to the result

$$\sigma'_D(\omega) = \epsilon_V \Delta\epsilon_D(\pi/2)(k_B T/E_H)\omega, \quad (16)$$

which is of the form of the Nowick et al. $B\omega$ term. But note that it is not of this form for all frequencies, and it is associated with a proper Kronig–Kramers real part. Eq. (16) leads to $\Delta\epsilon''(\omega) = \Delta\epsilon_D(\pi/2)(k_B T/E_H)$, where $\Delta\epsilon_D \equiv [\epsilon'_D(0) - \epsilon'_D(\infty)]$. If $\Delta\epsilon''(\omega)$ were constant at the value 0.03 over an appreciable frequency range [15], $T = 51.2$ K, and $E_H = 0.5$ eV, this expression would predict $\Delta\epsilon_D \simeq 2$, a reasonable value. Although the EDAE model can lead to power-law response over a wide frequency range, it can also yield more complex behavior at low relative frequencies, behavior needed to fit some of the present data (see Section 3.2).

3. $CaTiO_3$:30%Al^{3+} fitting results

3.1. Background and earlier slope estimates

Nowick and associates [6,17,18] have used frequency-response data of $CaTiO_3$:30%Al^{3+}, as well as that of several other materials, to illustrate and verify their new or 'second' universality. Some independent analysis of their $CaTiO_3$:30%Al^{3+} data sets has been carried out recently using a combination of CSD and DSD response [16]. It used the BDM response model to represent CSD and employed the EDAE model for DSD response. The BDM was used because it shows intrinsic $s(T)$ behavior with very few fitting parameters. Although this analysis made it clear that combined response was necessary to represent these data adequately, it was later found that better fits could be obtained with other CSD models than the BDM. Because the analysis to date of these data has either been overly simplistic or has been incomplete and unoptimized, I decided to carry out a detailed re-analysis of them over the available temperature range of 51.2 to 625.7 K using the CSD and DSD models described in the last section. Of particular importance is a comparison of such CNLS fitting results with the real-part ordinary-least-squares-fit results obtained by Nowick and associates using Eq. (3).

Although Nowick and associates state that the accuracy of their temperatures can be controlled to within 1 K [52], which might suggest rounding their temperature values to integers, it is a mistake to omit data which may be significant and whose omission might possibly bias results. Thus, in order to help obtain the best activation-energy estimates allowed by the data, I have used the original three- and four-figure temperature values without rounding. It is worth emphasizing that for an activation energy of 1.13 eV, Eq. (8) with K_C temperature-independent leads to values of $\rho'(0)$ at 50.7 and 51.7 K that differ from that for 51.2 K by factors of more than 12. Even at room temperature, a temperature difference of 0.5 K leads to more than a 7% change in $\rho'(0)$.

To set the stage, Fig. 1 compares four sets of slope and exponent results for this material, three of them representing previously published curves. The two BDM curves show actual slopes at $f = 10^5$ Hz, obtained using best-fit BDM parameters [16]. The other estimates are of exponents and so are averages over all or part of the available frequency range.

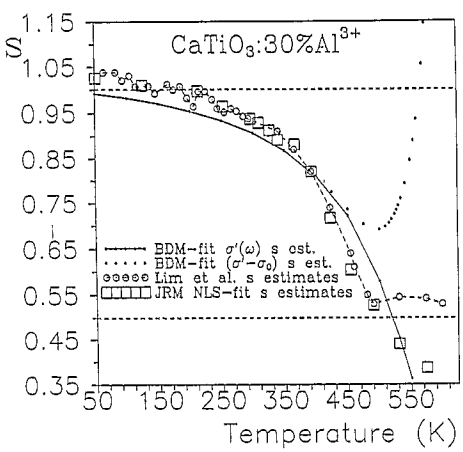

Fig. 1. Temperature variation of conductivity slope and power-law-exponent estimates, s and γ. The BDM points and line are actual log–log slope predictions of the model. The open-square points show power-law exponent values obtained from nonlinear-least-squares fits of $\sigma'(\omega)$ data.

Exponent values were obtained either by graphical estimation [6] or by ordinary least squares fitting, followed by the identification of the γ_0 of Eq. (3) (taking $B = 0$) or the γ of Eq. (10) (taking $\beta = 1$) with the effective slope. Jain and Hsieh [53] have published results similar to those of Fig. 1 (with $\gamma > 1$ at low temperatures) for a different glass than that of Fig. 1. Such similarity suggests that the methods of analysis applied herein might also be useful for analyzing their data as well.

First, we see that the solid-dot BDM slopes of $\Delta\sigma(\omega)$ disagree with the Lim, Vaysleyb and Nowick results [6,18], particularly at the high-temperature end where the BDM results begin to approach a slope of 2, which persists until the transition to a constant value of $\sigma'(\omega)$ in the high-frequency limit, behavior, required by physical realizability [38,50]. This limiting behavior appears at lower temperatures than is suggested by the data themselves, which do not extend to frequencies high enough to show such response. This comparison suggests that the BDM, and by extension, the GBEM model, is not universal.

In order to obtain results as close as possible to those of Nowick and associates for the present material, new NLS fits of $\sigma'(\omega)$ or $\epsilon''(\omega)$ were first carried out using the DSD Eqs. (13) and (14) for the lower temperatures, where the effects of $\sigma'(0)$ are entirely negligible. For such fitting with proportional weighing, the fits of data at the $\sigma(\omega)$ and $\epsilon(\omega)$ levels yield exactly the same parameter estimates and relative residuals [33,40,49]. The fit results are indicated by the open-square points in the figure Because the data do not extend to frequencies high enough to allow significant estimates of u_H to be obtained, large enough fixed values of this parameter were used so that increasing each value had no effect on the fit estimates.

Nowick and associates have questioned whether their low-temperature results, where $\gamma > 1$, should be taken seriously [18]. If one does so, they disagree with the 'new universality' hypothesis. This question has been addressed in Ref. [16] and is further answered below. Incidentally, complex or real-part fitting of the $\sigma(\omega)$ data using the CPE model did not, of course, yield slopes and exponents greater than unity. For the 51.2 K data, such fitting of the $\sigma'(\omega)$ data led, after very long iteration, to a value of the γ of Eq. (1) of unity to better than four decimal places, the upper limit of this quantity allowed by the model. Better and less restricted estimates are discussed later.

For the higher temperatures where $\sigma'(0)$ was sufficiently large to allow significant estimates of it to be obtained, the ZC CSD model of Eqs. (10) and (11) with $\beta = 1$ was used for fitting, with the estimates of γ taken as a measure of the slope. Although the open-circle points in Fig. 1 were almost certainly obtained graphically [6,18], their agreement with the present NLS results is good except at the highest temperatures. The reason for this discrepancy is discussed in Section 4.3.

3.2. Fitting of the low-temperature data

Before presenting CNLS-fit slope estimates, it is useful to look at the form of the data. Although the present data are noisy and have poor resolution, especially at low temperatures, and would be much improved for fitting purposes if they extended to both lower and higher frequencies with more points per decade, it is surprising how much can, nevertheless, be learned from them with CNLS analysis. Figs. 2–4 show data and fitting results for a low temperature, an intermediate temperature, and a high temperature.

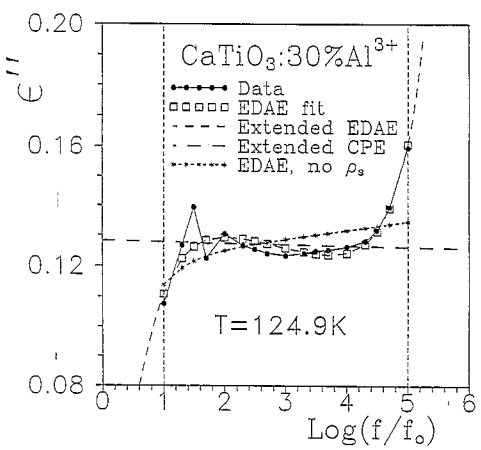

Fig. 2. Frequency dependence of 124.9 K $\epsilon'' = \Delta\epsilon''$ data and of various DSD CNLS fits to the data. The EDAE fit and the extended EDAE fit lines include the effect of a small series resistivity parameter, ρ_S. Here and elsewhere, f_0 is taken as 1 Hz, and the vertical dashed lines delineate the measured frequency range.

Once a good fit has been obtained at a given temperature, the fit parameters may be used to calculate the model predictions over a frequency range arbitrarily larger than that of the original data. Furthermore, since CNLS fitting may be expected to yield the most significant, objective values of the free fitting parameters, compared to any alternative approach, the best estimates of the effects of the various contributions to the total response can be individually calculated using only the relevant parameters [16]. This procedure is particularly helpful in obtaining $\Delta\sigma(\omega)$ in the low-frequency range where the estimate of $\sigma'(0)$ used in calculating this difference quantity becomes crucial, since other methods yield less accurate estimates for $\sigma'(0)$.

Fig. 2 for $\epsilon''(\omega)$ shows that the actual response differs appreciably from constant-loss data involving $\gamma_0 = 1$. At this low temperature, σ_0 plays a negligible role. The CPE curve shown is the best fit to the data of a model with such a 'new universality' value. Nowick and associates have suggested that a high-frequency increase apparent in their $CaTiO_3$:30%Al^{3+} and $Na_2O \cdot 3SiO_2$ data may be an experimental artifact. They state that "ϵ'' shows no systematic deviation from a constant value; however the last value, at 10^5 Hz, often shows an abrupt increase" [17]. The situation is more complicated: all their low-temperature data sets show a decrease at low frequencies and a sharp but smooth increase at the high end (one which certainly involves three or more points, not just the highest-frequency one), as in the present figure. Note that the decrease in ϵ'' at low frequencies is inconsistent with the simple power-law response function used by Nowick and his collaborators, but is well described by the EDAE model of Eq. (14), a model which can nevertheless predict a wide range of constant-slope behavior at higher frequencies.

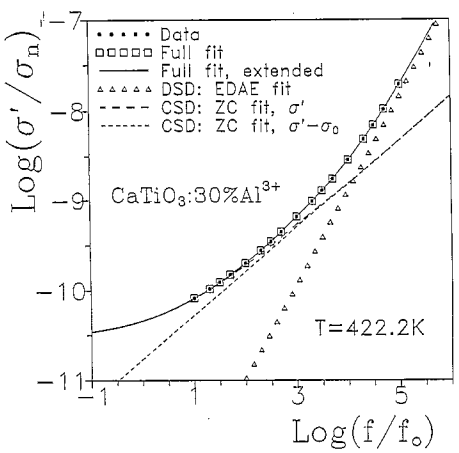

Fig. 3. Frequency dependence of 422.2 K $\sigma'(\omega)$ data and of a combined CSD and DSD CNLS fit to the data. Also shown are the responses of the various individual parts of the fit response. Here and elsewhere σ_n is taken as 1 $(\Omega\ \text{cm})^{-1}$.

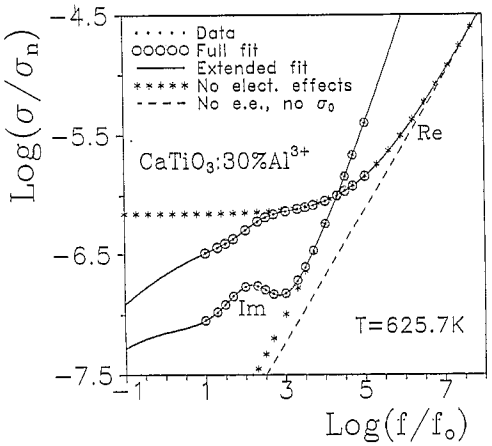

Fig. 4. Frequency dependence of 625.7 K $\sigma'(\omega)$ and $\sigma''(\omega)$ data and of a combined CSD and electrode-contribution CNLS fit to the data. Also shown are the responses of the various individual parts of the $\sigma'(\omega)$ fit response.

The high-frequency rise shown in Fig. 2 and present in the other low-temperature data sets involves systematic, non-random behavior. It has been found that this behavior can be well represented by a small resistance in series with the DSD EDAE response model. The figure compares fit results with and without such a series element, and it is clear that CNLS fitting allows an account for its effect, making it possible to obtain meaningful results for the DSD part of the response. The estimated series resistivity, ρ_S, varies slowly and monotonically from about 200 Ω cm at 51.2 K to about 286 Ω cm at 252.9 K. It is reasonably well determined: e.g., the relative error estimated from the CNLS fit of the series element at 51.2 K is less than 7%. Its temperature dependence can be adequately fitted with a linear equation in T, suggesting a thermal expansion effect. If we assume that the cell constant for the present data is 10 cm, then these results are consistent with a temperature-independent resistance, in series with the bulk of the

sample, of less than 20 Ω, although the linear thermal expansion coefficient required for full temperature independence is somewhat larger than expected. Although this small series element might arise from electrode resistance, it might alternatively be associated with the measuring apparatus itself. Simple experiments could readily resolve this uncertainty. Whatever the genesis of the series element, its identification and inclusion in the fitting model is important, since doing so allows one to eliminate its effect on the bulk response of the material and, concomitantly, shows how more accurate than otherwise high-frequency results may be obtained from the measuring equipment.

The Fig. 2 curve with open-square points shows how well the EDAE model plus a series resistive element fits the data. For a perfect fit, the squares would evenly enclose the solid data points. The actual ϕ estimate obtained from this fit was 0.0217 $\pm$ 0.0045. Here and elsewhere, the uncertainty listed is that of a single standard deviation, and similar values are obtained for the other low-end fits. The relative uncertainties of these ϕ estimates are small enough that they can be unambiguously distinguished from 0, and so they do not support the assumption of a temperature-independent exponent of unity ($\phi = 0$).

For comparison, the EDAE-fit results without ρ_S do not agree as well with the data and involve a much more uncertain ϕ estimate of about -0.01 ± 0.006, leading to the exponent estimate of about 1.01 shown for this temperature in Fig. 1. Thus, it seems likely that exponent values which exceed unity in Fig. 1, as well as others showing such behavior (e.g., [13,14,53]), arise because the data used for their determination, whether graphical or NLS fitting, included the influence of ρ_S, but its effects were not explicitly accounted for in the fitting model. Thus, in the absence of more careful analysis, they should not be interpreted as indicating the presence of a dispersion process with $\gamma \geq 1$, and the present results therefore do not support the new universality hypothesis. More discussion of the low-temperature fitting results is included in Section 4.2.

3.3. Fitting of intermediate-temperature data

In the temperature range 270 K $< T <$ 510 K, the data could best be fit by combined CSD and DSD response, Eq. (9). No ρ_S parameter was needed; Eqs. (10) and (11) with $\beta = 1$ were used for CSD response; and Eqs. (13) and (14) were employed for DSD response. In addition, in all present CNLS fitting, $\epsilon_\infty = \epsilon_{C\infty} + \epsilon_{D\infty}$ was taken as a free fitting parameter. Within the uncertainties of the data, it was found to be substantially temperature independent and close to 60. Although simultaneous fitting of both $\sigma'(\omega)$ and $\sigma''(\omega)$ data is crucial to getting an optimized and adequate fit of the data, especially when several different processes are involved as in Eq. (9), only the $\sigma'(\omega)$ part of the combined CNLS fitting is shown here because $\sigma''(\omega)$ curves usually show somewhat less detail in this temperature range.

Typical intermediate-range data and fit results are presented in Fig. 3; as usual, the fit results have been extended on either side of the actual data range. Note that the full-fit points are indistinguishable from the corresponding data points. As mentioned earlier, one of the advantages of CNLS fitting is that the resulting parameter estimates may be used to predict the responses of the CSD and DSD processes separately at any immittance level [16]. The figure shows that the CSD part of the response is dominant up to $\sim 10^3$ Hz and the DSD becomes important above $\sim 10^4$ Hz. The fit estimates of γ and $1 - \phi$ were 0.488 ± 0.006 and 1.046 ± 0.009, respectively. The standard deviation of the relative residuals of the present fit, S_F, was about 0.003, indicating an excellent fit of the data. For comparison, the fit using Eq. (10) with $\gamma = 1$ and β free to vary, led to $\beta \simeq 0.406 \pm 0.007$ and $S_F \simeq 0.006$. Besides yielding a substantially poorer fit, this model also led to a less consistent estimate of $\sigma'(0)$ than did the ZC fit.

Jain and Hsieh [53] have recently considered the effect of the width of the available frequency window on estimates of power-law exponents of $\sigma'(\omega)$ CSD data fitted using NLS. Define $w(f_{max})$ as the ratio $\sigma'(f)/\sigma'(0)$, where $f = \omega/2\pi$. Using sodium aluminosilicate glass data, they have shown that as w decreases and the dc plateau becomes a larger and larger part of the window range, the estimated γ increases [53]. Although these authors seem to suggest that this is a general result, simulation results with actual power-law data similar to that presented in Ref. [53] indicate otherwise. In general, in the absence of systematic errors, one would expect windowing effects to depend on the number and spacing

of the points in the window, on the type of random errors present, and on the type of fitting used. Some pertinent results are presented below.

Data were formed by adding 2% independent, normally distributed errors to both the real and imaginary parts of exact power-law response which involved a value of $\epsilon_{D\infty}$ of 7. The original exact $\sigma(\omega)$ data, extending from 50 to 10^5 Hz with 10 points/decade equally spaced in $\log(\omega/\omega_n)$, involved $\gamma = 0.67$ and $w(10^5) = 8.9$. CNLS fitting with proportional weighing of the full noisy data yielded an estimate for γ of about 0.683 ± 0.005, while fitting with the $w(10^4) = 2.7$ window led to $\gamma \simeq 0.664 \pm 0.010$. Finally, for $w(10^3) = 1.3$, $\gamma \simeq 0.588 \pm 0.050$. Separate real-part (as in Ref. [53]) and imaginary-part fitting led, respectively, to results for the three window widths of 0.693 ± 0.012, 0.683 ± 0.020, and 0.688 ± 0.147; and 0.681 ± 0.011, 0.655 ± 0.025, and 0.604 ± 0.107. We see that although the CNLS uncertainties are appreciably smaller than those for the other fits, there is no apparent tendency for γ to increase as w decreases, even for the real-part fitting. Next, similar exact data to the above were produced with $10 \leq f \leq 10^3$ Hz and 40 points/decade. From this set, data sets with three different sizes of random errors were then constructed. Fitting estimates of γ for the CNLS and real-part fits of the 0.5, 1, and 2% error data sets yielded, respectively, 0.668 ± 0.002, 0.667 ± 0.004, and 0.663 ± 0.008; and 0.748 ± 0.047, 0.835 ± 0.083, and 1.0 ± 0.17. Note that only the minus sign is operative in ± 0.17 since the fit model does not allow $\gamma > 1$. These last results show a slight decrease of the CNLS γ estimates with increasing error relative standard deviation, but a strong increase in the estimates obtained with real-part fitting. It is thus quite clear that CNLS fitting is much superior to real- and imaginary-part fitting for noisy power-law data of the present types. The present results provide further justification for the use throughout this work of CNLS rather than NLS fitting.

The above results provide one with some idea of what to expect when fitting the ZC power-law model to experimental data for which it is the proper (or inappropriate) model. It is thus of interest to investigate windowing effects for the present experimental data. Is the power-law approach indeed the most appropriate for these data? CNLS fits at the complex conductivity level of the 393.2 K experimental data [17] were carried out for the ZC, KWW0, and KWW1 models with $w(10^5) \simeq 4720$ and $w(10^3) \simeq 88$. At this temperature, no electrode effects were significant. First, it was found that all fits were good and that there was negligible difference between the CSD exponent estimates for these two windows for all three models. For example, for the ZC, γ estimates of 0.500 and 0.492 were obtained. Second, the degree of fit was negligibly different between the three models, indicating that any of them would be satisfactory. The values of β found for the KWW0 and KWW1 fits, β_0 and β_1, were $\beta_0 = 0.490$ and 0.485 for the two windows, and $\beta_1 = 0.517$ and 0.530, respectively. We see that the expected relations $\beta_0 \simeq 1 - \beta_1 \simeq \gamma \simeq s$ are approximately satisfied. The ϕ estimates for the full-data fits using the three models were about -0.051 using the ZC and KWW0 models, and -0.048 for the KWW1. Finally, parameter estimates and degree of fit were essentially indistinguishable for fitting with proportional weighing of the data at the modulus level and at the complex conductivity level, again indicating that all the models can represent the data exceptionally well. To distinguish between them at this temperature, it would be necessary to use more accurate data with an appreciably wider frequency span.

3.4. Fitting of high-temperature data

Fig. 4 shows fitting results of the highest-temperature data available for the present material. Here the data and fit results are shown for both the real and imaginary parts of the conductivity. The individual S_F values for the real and imaginary parts of the CNLS fit were 0.007 and 0.011, respectively, indicating that few relative residuals exceeded 1%. Define a value of σ/σ_n as V. Then $V_{fit} = V_{data} + R$, where R is here the residual for the selected point. If $|r| \equiv |R/V_{data}| \ll 1$ the situation for the present fits, then $\log(V_{fit}) \simeq \log(V_{data}) + r\log(e)$ where r is the relative residual. Since r is of the order of 1% for the fits of Fig. 4, it is clear why 'error' bars for the fit points are too small to show up there, and a better indication of the adequacy of fit is the degree to which the open-circle fit points are centered on the data points.

Particularly significant in Fig. 4 are the large

low-frequency electrode contributions. Their influence is not entirely limited to low frequencies alone, and it continues to be non-negligible to 10^5 Hz or above for the present data. In the temperature range where good fitting required the presence of additional parameters to account for such electrode contributions, it was found that their estimated values depended somewhat on temperature but eventually decreased toward zero as the temperature decreased.

In order to obtain adequate CNLS fits, electrode contributions had to be included, as in Eq. (9), for all temperatures above 460 K. At this end of the temperature range, it was found that they could usually be represented by a capacitor and a CPE in parallel, all in series with the parallel combination of CSD and DSD response contributions. This combination has also been found appropriate for representing electrode effects in the response of a Li_2O–Al_2O_3–$2SiO_2$ glass [40]. The value of the capacitor required for the present material remained constant within a factor of two in the range 531.2 K $\leq T \leq$ 625.7 K. At $T =$ 625.7 K, the further addition of a series resistance improved the fit by yielding an estimate of $\sigma'(0)$ in better agreement with values for nearby temperatures than that obtained without such an addition, but no such element improved the fit for lower temperatures. With the resistor present, S_F was 0.008, and it increased to 0.012 without this element, but its presence or absence had only minimal effect on the other parameters. With no electrode effects included in the fitting model, it was found that at 625.7 K the ZC model did not lead to a converged fit at all. Thus, a power-law CNLS fit could not be obtained unless electrode contributions were explicitly accounted for.

Electrode effects clearly lead to a peak in the $\sigma''(\omega)$ response in the low-frequency region for the data of Fig. 4. It disappears when the response is calculated from the final values of the fitting parameters without including the electrode elements. The figure shows both $\sigma'(\omega)$ response and $\Delta\sigma(\omega)$ response with all electrode effects eliminated in this way. Note that the power-law contribution, whose exponent is here about 0.56 ± 0.02, only begins to dominate the CSD part of the response beyond the highest measurement frequency. Therefore, graphical estimation of the exponent from the available data would be uncertain, and even the present CNLS estimate is likely to be considerably more uncertain than indicated above — principally because of uncertainty in finding an appropriate model for the electrode contributions.

Windowing effects [53] are more important for the present high-temperature range than for lower temperatures because with a fixed measuring frequency range from 10 to 10^5 Hz, the higher the temperature the less of the final rise of $\sigma'(\omega)$ at high frequencies falls within the available range. Consider fitting results at $T = 531.2$ K, where $w(10^5) \simeq 9.6$, and for $w(5 \times 10^3) \simeq 3$. CNLS fitting of $\sigma(\omega)$ data using the ZC, KWW0, and KWW1 CSD models over the full frequency range yielded S_F values of 0.009, 0.0124, and 0.029, respectively, showing that the ZC was superior to the other models. For fitting only up to 5000 Hz, the values found were 0.007, 0.027, and 0.055, respectively, using the same electrode parameter values obtained for the full-range ZC fit. The estimates of γ, β_0 and β_1 for the large and small values of w were, respectively, 0.485, 0.429, and 0.614, and 0.494, 0.343, and 0.573. The β values and their changes, as well as the corresponding S_F values, show that the KWW models are appreciably inferior to the ZC one at this temperature. The slight increase, rather than decrease, in γ as the range is decreased possibly indicates that the CSD part of the data is not perfectly modeled by even the ZC. Because of the appreciable contribution of electrode effects at this and higher temperatures, which themselves must be modeled perfectly before even the most appropriate CSD model can yield entirely proper fitting, the present small discrepancy is not unexpected, however, and it does not necessarily indicate that the ZC is not a proper CSD fitting model for these data.

4. Temperature dependencies of fitting parameters

4.1. Overall slope estimates and background

The results of the present work which are most relevant to universality or its absence appear in Fig. 5. First, we see the regions over which DSD and CSD models were useful in fitting the data. Both regions are here limited, but, I believe, only by the finite resolving power of CNLS fitting and the relatively narrow frequency range of the available data.

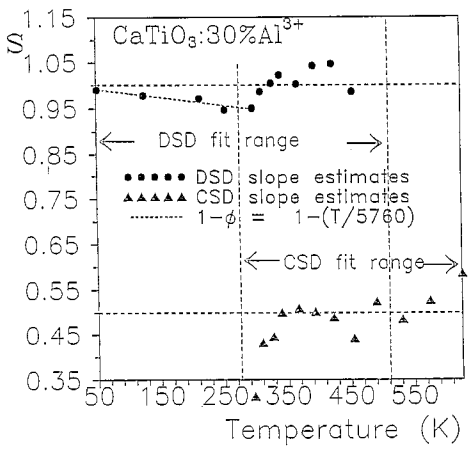

Fig. 5. Temperature dependencies of DSD and CSD log–log slope estimates obtained from CNLS fitting involving an exponential-distribution-of-activation-energies model for DSD and a power-law one for CSD.

With data extending over a wider, but still finite frequency range, one would expect to be able to follow DSD response to higher temperatures and to identify CSD behavior to lower ones. But even then, at sufficiently high temperatures the DSD contribution would eventually become too small compared to the other parts of the data to allow its estimation, and similarly at low temperatures for the CSD part of the total. There seems to be no suggestion in the data that, in principle, these separate contributions only apply in limited temperature regions — they just become too small, comparatively, to analyze.

Instead of presenting results like those shown in Fig. 5, Nowick and associates assumed an ab initio DSD power-law exponent of unity and quote a value for the γ_0 of Eq. (3) of 0.55 for the present material [18]. They state that there is no evidence for the dependence of γ on temperature over the entire temperature range of the experiment, so the value 0.55 should apply over that full range. But their results are based on graphical and least squares analysis of only the $\sigma'(\omega)$ data and thus are more uncertain and do not yield the detailed estimates shown in Fig. 5.

4.2. DSD results

I conclude from the results shown in Fig. 5 that for the present data, the first universality is alive and well: power-law response is endemic, certainly not surprising. Further, the third universality, which may now be defined as a combination of CSD and DSD responses, each with its own nearly temperature-independent γ values of less than unity, also appears plausible. But there is more to be concluded. The presence of well-defined Eq. (2) response for the DSD exponent in the range 51.2 K $\leq T \leq$ 296.2 K indicates that when the data are more completely analyzed the $\gamma_0 = 1$ 'second universality' posited by Nowick and associates disappears, as already suggested earlier on less evidence [16]. Incidentally, the T_0 value listed in Fig. 5 corresponds to an activation energy of about 0.5 eV.

But what about the higher-temperature DSD exponent estimates? Those with $\gamma \geq 1$ only appear in the combined DSD–CSD fitting region and may be expected to become less and less accurate as the temperature increases. In fact for $T = 490.2$ K, the $1 - \phi$ estimate was about 1.3, and DSD fitting was impossible for higher temperatures. Thus, while the data do not suggest that the exponent cannot be larger than unity for the higher temperature range, it would be conservative to conclude on the basis of the more accurate lower-temperature results that it is not. Finally, it should be reiterated that the thermally activated EDAE DSD response model predicts just the behavior exemplified by Eq. (2) and illustrated in Fig. 5 by the fit results over the DSD-dominant temperature range [9,12].

If the DSD response is indeed thermally activated, as suggested by its Eq. (2) response, it is necessary that τ_D satisfy an equation like Eq. (6) with an E_H value appropriate for DSD response. But once τ_D becomes large, so $\Omega_D \gg 1$, Eq. (16) shows that it no longer plays an active role in the response when $\phi = 0$. Similar behavior applies for the ϕ values near 0 involved in the present DSD response. It thus turns out to be impractical to obtain good estimates from the present data of the τ_D thermally activated parameters. All one can conclude is that $\tau_D \ll 1$ in the low-temperature region and it is $\gg 1$ in the high-temperature region. Nevertheless, the evidence suggests that it is indeed thermally activated, certainly a possibility for DSD [54,55].

There is no need for $\Delta\epsilon_D$ to be thermally activated, nor should it be expected to be since independent dipoles lead to T^{-1} Curie-law behavior [54].

Unfortunately, it is impossible to estimate the u_H parameter of Eq. (14) from the present limited high-frequency data, and, as Eq. (16) indicates, fitting can then only provide an estimate of the combined quantity $\Delta\epsilon_D/u_H$. If one selects any reasonable temperature-independent value for $E_{DH} \equiv E_H$, estimates of $\Delta\epsilon_D$ may be calculated from the fit results, and they turn out to be nearly independent of temperature, within a reasonable random variation, for the range $51.2\ \text{K} \leq T \leq 296.2\ \text{K}$ and even somewhat higher.

4.3. CSD results

The middle CSD exponent estimates in Fig. 5 evidently tend to cluster around a value of 0.5. The increasing trend of γ in the upper range where no DSD fit is possible may arise just because as the temperature increases there is progressively less and less useful high-frequency data available to estimate γ adequately. Likewise, the sharp drop below 339.7 K is likely only to be a consequence of the difficulty of resolving small CSD contributions in the presence of much larger DSD ones. Incidentally, the differences between the exponent values above 490 K in Fig. 1 and those in Fig. 5 arise because the Fig. 5 fits include electrode effects as required and those shown in Fig. 1 do not.

The CNLS fits of the data allowed $\rho'(0)$ to be a free fitting parameter in the range $422.2\ \text{K} \leq T \leq 625.7\ \text{K}$. The resulting values led to the following estimates of E_ρ from untransformed NLS fitting with Eqs. (7) and (8), respectively: 1.174 ± 0.017 eV and 1.130 ± 0.016 eV. Nowick and associates obtained the surprisingly larger value of 1.22 eV, but did not specify their actual fitting formula or method [18]. The Eq. (7) fit also gave a τ_a estimate of 1.1×10^{-15} s while that of Eq. (8), taking K_C as a constant, yielded $\tau_a/K_C \simeq 1.1 \times 10^{-16}$ s. As discussed below, there is good evidence that K_C is indeed temperature independent and approximately equal to 36. Then the Eq. (8) prediction of τ_a is about 4×10^{-15} s. The above Eq. (8) estimate for E_ρ implies that there is approximately a 68% probability that its value lies in the range $1.114\ \text{eV} \leq E_\rho \leq 1.146\ \text{eV}$, equivalent to an uncertainty of about $\pm 1.4\%$. For comparison, the Nowick estimate differs from the two present estimates by about 4% and 8%, respectively, implying no overlap, even at the 95% probability level. I believe that the present values, which are based on CNLS estimates of $\rho'(0)$ having estimated relative standard deviations of 1% or less, are to be preferred to those obtained by graphical methods, which may lead to uncertainties of 10% or more, perhaps a reason why no such uncertainties are usually quoted.

Incidentally, fitting of logarithmically-transformed data leads to bias in problems of the present type [56]. The range of possible CSD fitting was extended below 422.2 K by using fixed values of $\rho'(0)$ calculated from Eq. (7) with the above parameter values. No significant differences were obtained using Eq. (8) instead. This procedure is, of course, another source of uncertainty in the results, particularly for the lower three temperatures, but it allows CSD estimates to be obtained at temperatures where CNLS fitting does not lead to significant and plausible $\rho'(0)$ values.

The result that most of the middle-temperature CSD γ estimates are quite close to 0.5 is strongly suggestive of a diffusion process. Therefore, some fits were carried out using the ordinary finite-length Warburg diffusion model, often observed in ionic CSD systems [39,57], rather than the ZC model. The signature of this response is an exponent value of 0.5, but it is quite unsymmetric and led to much poorer fits.

Another fitting possibility might be thought to be the diffusion-controlled relaxation model (DCRM) for ionic transport in glasses [58]. It has indeed been suggested as a possible fitting model by Nowick and associates [18], where it is implicitly identified as a CSD response theory by the present definition of conductive-system dispersion. It too can lead to an exponent near 0.5, but it seems inapplicable to the present situation because it was derived as a dielectric response model; does not yield a dc conductivity; and so represents DSD rather than CSD response.

Contrary to an earlier assertion [18], the ac and dc conductivities of a system where the DCRM applies are not necessarily parts of the same interactive ion-jumping process. The DCRM involves diffusion between two neighboring negatively charged (possibly non-bridging oxygen) sites. Even if the dc conductivity of the material is taken proportional to a diffusion constant [58], it must involve percolation through the entire material or else it is zero, and it is

thus most unlikely to be directly related to local DCRM response, which does not require such percolation. Although the DCRM might be transformed to CSD response by formally changing $\epsilon_D(\omega)$ quantities to $\rho_C(\omega)$ ones [9], new physically-based justification would then be required. In any event, it appears more likely that the ZC γ parameter is a constant of 0.5 rather than the value of 0.55 obtained earlier [18].

Finally, what can one learn from the fit estimates of the $\epsilon_{C\tau}$ parameter of Eqs. (11) and (12)? Rounding off values, it was found to be 34, 30, 37, 42, 35, and 36 for temperatures of 625.7, 574.7, 531.2, 490.2, 454.2, and 422.2 K, respectively. These results indicate that $\epsilon_{C\tau} \simeq 36$ and is neither thermally activated nor proportional to T^{-1}, and they suggest that it is actually most likely to be temperature independent. If so, Eq. (12) indicates that K_C, which is not thermally activated, is itself constant, and the temperature dependencies of $\rho'(0)$ and τ_C are the same and involve no power of T in their pre-exponential factors. Then Eq. (8) should be preferred to Eq. (7). For comparison, Nowick and associates obtained an estimate of their E_τ of 1.25 eV [18], considerably different from the present Eq. (8) $E_\rho = E_\tau$ estimate of 1.13 eV.

At temperatures below 422 K, where the appropriate values of $\rho'(0)$ are more uncertain, it is possible to obtain a value of $\epsilon_{C\tau}$ of 36 by using somewhat smaller values of $\rho'(0)$ than those predicted by the fit of higher-temperature $\rho'(0)$ estimates. For $T =$ 393.2 K and 366.7 K, the predicted values yield $\epsilon_{C\tau} \simeq 49$ and 77, respectively, while the values obtained when $\rho'(0)$ was allowed free to vary were 19 and 23, respectively. Even these more uncertain $\epsilon_{C\tau}$ estimates still suggest, however, that $\epsilon_{C\tau}$ is likely to be substantially independent of temperature for the present data.

For many materials, it is common to find that $\epsilon'(\omega)$ increases rapidly down to the lowest measured frequencies [40,59]. Very large values are observed, especially at higher temperatures. For example, the experimental value of $\epsilon'(\omega)$ at 625.7 K and 10 Hz for the present material is about 1.6×10^4. Most of this behavior arises from electrode polarization effects, since at $T = 422.2$ K, where such effects seem to be negligible, $\epsilon'(\omega)$ is about 73 at this frequency and is also still increasing with decreasing frequency. In the absence of electrode effects, one can write for the combined CSD and DSD contributions [40],

$$\epsilon'(0) = \epsilon_{C0} + \epsilon'_D(0) = \epsilon_{C\tau}\langle x\rangle + \epsilon'_D(0), \qquad (17)$$

where here $\epsilon'_D(\omega)$ may be taken as $\epsilon_{D\infty}$ in the absence of DSD in the measured frequency range. Because the ZC model is physically unrealistic in the limit of low frequencies [38], it cannot be used to estimate ϵ_{C0}. But fits with other models, such as the Cole–Davidson model, which do not suffer from this limitation, suggest that ϵ_{C0} is of the order of 60 at 422.2 K.

5. Summary and conclusions

The present work is concerned both with the description of data analysis methods heretofore little used in the disordered materials area and with the results of their application to data sets of Nowick and associates which have been employed by them to propose and justify the existence of a constant-loss new universality.

The main analysis method used herein is complex non-linear least squares fitting of frequency-response data using proportional weighing, weighing which does not emphasize peaks of the data at the expense of the rest of the data, as does conventional unity weighing [33,49]. CNLS fitting of both real and imaginary parts of the data simultaneously is shown to be more appropriate than the conventional approach of fitting $\sigma'(\omega)$ data alone, usually carried out with ordinary least squares fitting or graphically. An important virtue of the CNLS approach is its objective character: it has tremendous resolving power (one part in a million or better for good data [33]) and thus allows all processes contributing to the response, such as conductive-system dispersion, dielectric-system dispersion, the high-frequency-limiting dielectric constant, dc conductivity, and any electrode polarization effects present, to be identified and quantified. In addition, it not only provides a statistical measure of the goodness of fit of the analysis, but estimates of all parameters and their standard deviations as well. These uncertainty estimates are an essential aid in assessing the importance of the various contributions to the full response but have been rarely provided in previous work.

Finally, CNLS fitting of appropriate models allows one to obtain the fit response of the system with or without any of the above individual contributions, over a frequency range which may exceed that of the original data.

CNLS fitting of the $CaTiO_3$:30%Al^{3+} dispersion data of Nowick and associates led to the following significant results. First, it was verified objectively, rather than assumed ab initio, that the response could be best represented by a combination of DSD and CSD processes, rather than by a single dispersion process involving complicated slope dependence on temperature. Second, a plausible explanation has been found for the slope estimates greater than unity published previously for the present data at low temperatures [6,18], allowing the problem to be avoided herein. Next, the analysis showed, contrary to previous conclusions based on less appropriate methods and an inadequate fitting model, that the dielectric dispersion does not involve a constant-loss region at low temperatures, one assumed by the form of the Nowick-and-associates analysis model. Instead of yielding a temperature-independent frequency exponent of unity consistent with such loss, the analysis led to a clearly defined temperature dependence of $1-(T/T_0)$ over the region 51 K $< T <$ 297 K, agreement with many previous theoretical analyses and consistent with the specific thermally-activated distribution-of-activation-energies model used for fitting the DSD part of the total response. The uncertainties in the estimated points defining this dependence were sufficiently small that it could be unambiguously distinguished from a constant value of unity. Thus, although the new universality proposed by Nowick and associates was not verified for this material, the response seems likely to involve a thermally activated distribution of activation energies.

For the CSD part of the response, it was found that estimates of the frequency exponent yielded values close to 0.5 over the range 339 K $< T <$ 423 K, that where the exponents could be most accurately determined. The value of 0.5 is suggestive of a diffusion process, and it could be accurately discriminated from the value of 0.55 cited by Nowick and associates.

The analysis showed that electrode polarization effects needed to be added to the total fitting model for temperatures of 460 K and above in order to obtain adequate fits of the data. Such polarization was found to affect not only the low-frequency end of the data range but, contrary to usual expectations, the high-frequency one as well [40].

A sensitive differential method of distinguishing between the activated temperature dependencies of the dc resistivity, $\rho'(0)$, and the relaxation time of a CSD response model, τ_C, was proposed and illustrated using CNLS fitting. It led to a well-defined activation energy estimate of 1.130 ± 0.016 eV for both $\rho'(0)$ and τ_C, appreciably different from the values of 1.22 eV and 1.25 eV cited by Nowick and associates for these quantities [18], and sufficiently well determined that the present and Nowick values are unlikely to overlap even within the largest likely uncertainties of these quantities. The ratio $\tau_C/\rho'(0)$ was found to be essentially temperature independent and not thermally activated, indicating more clearly than previously that no T factor occurs in the pre-exponential term of the $\rho'(0)$ Arrhenius temperature expressions, since none occurs in the conventional τ_C one.

The present results demonstrate that the CNLS data analysis method, which is readily available in the LEVM fitting program [33], can lead to more appropriate fitting results than can other less objective methods. Since more accurate and better resolved results help one to gain new physical insights into the behavior of the material analyzed, it seems clear that the CNLS approach should be more widely applied in future for glasses and other disordered materials.

6. Principal acronyms and subscripts

ac	Alternating current.
BDM	Bryksin, Dyre, Macdonald CSD effective-medium response model.
BNN	Barton, Nakajima and Namikawa equation.
C	Subscript denoting conductive.
CNLS	Complex non-linear least squares.
CPE	Constant-phase distributed circuit element.
CSD	Conductive-system dispersion.
D	Subscript denoting dielectric.
dc	Direct current.
DCRM	Diffusion-controlled relaxation model.

DSD Dielectric-system dispersion.
EDAE Exponential distribution of activation energies.
GBEM Generalized Bryksin (BDM) effective-medium CSD response model.
LEVM The CNLS fitting program used herein.
NLS Non-linear least squares.
S_F Standard deviation of the relative residuals of a NLS or CNLS fit.
ZC Cole–Cole DSD response model used at the impedance level for CSD response.

References

[1] A.K. Jonscher, Nature (London) 256 (1975) 566.
[2] A.K. Jonscher, Nature (London) 267 (1977) 673.
[3] K.L. Ngai, Comments Solid State Phys. 9 (1979) 127; 9 (1980) 141.
[4] R. Kohlrausch, Pogg. Ann. Phys. Chem. 91(2) (1854) 179; G. Williams and D.C. Watts, Trans. Faraday Soc. 66 (1970) 80.
[5] W.K. Lee, J.F. Liu and A.S. Nowick, Phys. Rev. Lett. 67 (1991) 1559.
[6] B.S. Lim, A.V. Vaysleyb and A.S. Nowick, Appl. Phys. A56 (1993) 8.
[7] S.R. Elliott, Philos. Mag. 36 (1977) 1291.
[8] A.R. Long, Adv. Phys. 31 (1982) 553.
[9] J.R. Macdonald, J. Appl. Phys. 58 (1985) 1955, 1971.
[10] S.R. Elliott, Adv. Phys. 36 (1987) 135.
[11] M.P.J. van Staveren, H.B. Brom and L.J. de Jongh, Phys. Rep. 208 (1991) 1.
[12] J.R. Macdonald and J.C. Wang, Solid State Ionics 60 (1993) 319.
[13] G. Balzer-Jollenbeck, O. Kanert, J. Steiner and H. Jain, Solid State Commun. 65 (1988) 303; X. Lu and H. Jain, J. Phys. Chem. Solids 55 (1994) 1433.
[14] R.H. Cole and E. Tombari, J. Non-Cryst. Solids 131–133 (1991) 969.
[15] J.R. Macdonald, J. Appl. Phys. 75 (1994) 1059.
[16] J.R. Macdonald, Appl. Phys. A59 (1994) 181.
[17] A.S. Nowick, A.V. Vaysleyb and B.S. Lim, J. Appl. Phys. 76 (1994) 4429.
[18] A.S. Nowick, B.S. Lim and A.V. Vaysleyb, J. Non-Cryst. Solids 172–174 (1994) 1243.
[19] S.R. Elliott, Solid State Ionics 70&71 (1994) 27.
[20] J.R. Macdonald, J. Electroanal. Chem. 378 (1994) 17.
[21] M. Pollak and G.E. Pike, Phys. Rev. Lett. 28 (1972) 1449.
[22] J.C. Wang and J.B. Bates, Solid State Ionics 50 (1992) 75.
[23] G. Frossati, R. Maynard, R. Rammal and D. Thoulouze, J. Phys. Lett. (Paris) 38 (1977) L-153.
[24] D.L. Sidebottom, P.F. Green and R K. Brow, Phys. Rev. Lett. 74 (1995) 5068.
[25] A. Hunt, J. Non-Cryst. Solids 160 (1993) 183.
[26] J.C. Dyre, Phys. Rev. B48 (1993) 12511.
[27] V.V. Bryksin, Fiz. Tverd. Tela (Leningrad) 22 (1980) 2441 [Sov. Phys. Solid State 22 (1980) 1421].
[28] J.R. Macdonald, Phys. Rev. B49 (1994-II) 9428.
[29] S.R. Elliott and F.E.G. Henn, J. Non-Cryst. Solids 116 (1990) 179.
[30] R. de L. Kronig, J. Opt. Soc. Am. 12 (1926) 547.
[31] H.A. Kramers, Atti Congr. Fisici, Como (1927) 545; Phys. Z. 30 (1929) 52.
[32] J.R. Macdonald, Phys. Lett. A, to be published.
[33] J.R. Macdonald and L.D. Potter Jr., Solid State Ionics 23 (1987) 61; J.R. Macdonald, J. Electroanal. Chem. 307 (1991) 1.
[34] D.P. Almond and A.R. West, Solid State Ionics 9&10 (1983) 277.
[35] J.R. Macdonald and G.B. Cook, J. Electroanal. Chem. 193 (1985) 57.
[36] S.R. Elliott, Solid State Ionics 27 (1988) 131.
[37] T.S. Havriliak and S. Negami, J. Polym. Sci. C14 (1966) 99.
[38] J.R. Macdonald, Solid State Ionics 25 (1987) 271.
[39] J.R. Macdonald, ed., Impedance Spectroscopy – Emphasizing Solid Materials and Systems (Wiley-Interscience, New York, 1987).
[40] J.R. Macdonald, J. Non-Cryst. Solids 197 (1996) 83.
[41] P.B. Macedo, C.T. Moynihan and R. Bose, Phys. Chem. Glasses 13 (1972) 171.
[42] C.T. Moynihan, L.P. Boesch and N.L. Laberge, Phys. Chem. Glasses 14 (1973) 122.
[43] J.R. Macdonald and R.L. Hurt, J. Chem. Phys. 84 (1986) 496.
[44] R.H. Doremus, Glass Science, 2nd Ed. (Wiley-Interscience, New York, 1994) p. 296.
[45] J.L. Barton, Verres Refract. 20 (1966) 328.
[46] T. Nakajima, in: 1971 Ann. Rep., Conf. on Electric Insulation and Dielectric Phenomena (National Academy of Sciences, Washington, DC, 1972) p. 168.
[47] H. Namikawa, J. Non-Cryst. Solids 18 (1975) 173.
[48] C.P. Lindsey and G.D. Patterson, J. Chem. Phys. 73 (1980) 3348.
[49] J.R. Macdonald, J. Chem. Phys. 102 (1995) 6241.
[50] B.A. Boukamp and J.R. Macdonald, Solid State Ionics 74 (1994) 85.
[51] J.R. Macdonald, J. Appl. Phys. 61 (1987) 700.
[52] W.K. Lee, B.S. Lim, J.F. Liu and A.S. Nowick, Solid State Ionics 53–56 (1992) 831.
[53] H. Jain and C.H. Hsieh, J. Non-Cryst. Solids 172–174 (1994) 1408.
[54] P.K. Dixon, Phys. Rev. B42 (1990) 8179.
[55] F. Stickel, E.W. Fischer and R. Richert, J. Chem. Phys. 102 (1995) 6251.
[56] W.J. Thompson and J.R. Macdonald, Am. J. Phys. 59 (1991) 854.
[57] D.R. Franceschetti, J.R. Macdonald and R.P. Buck, J. Electrochem. Soc. 138 (1991) 1368.
[58] S.R. Elliott and A.P. Owens, Philos. Mag. B60 (1989) 777.
[59] A.R. Long, J. McMillen, N. Balkan and S. Summerfield, Philos. Mag. B58 (1988) 153.